Title

X-Ray Energy Dispersive Spectroscopy of Intergranular Phases in β11 β' Sialons

Authors

Dinger, T R
Thomas, G

Publication Date

1982-09-01

Lawrence Berkeley Laboratory
UNIVERSITY OF CALIFORNIA

Materials & Molecular Research Division

Presented at the Advances in Materials Characterization Conference, University Series on Ceramic Science, Alfred University, Alfred, NY, August 16-18, 1982

X-RAY ENERGY DISPERSIVE SPECTROSCOPY OF INTERGRANULAR PHASES IN β11 β' SIALONS

T.R. Dinger and G. Thomas

September 1982

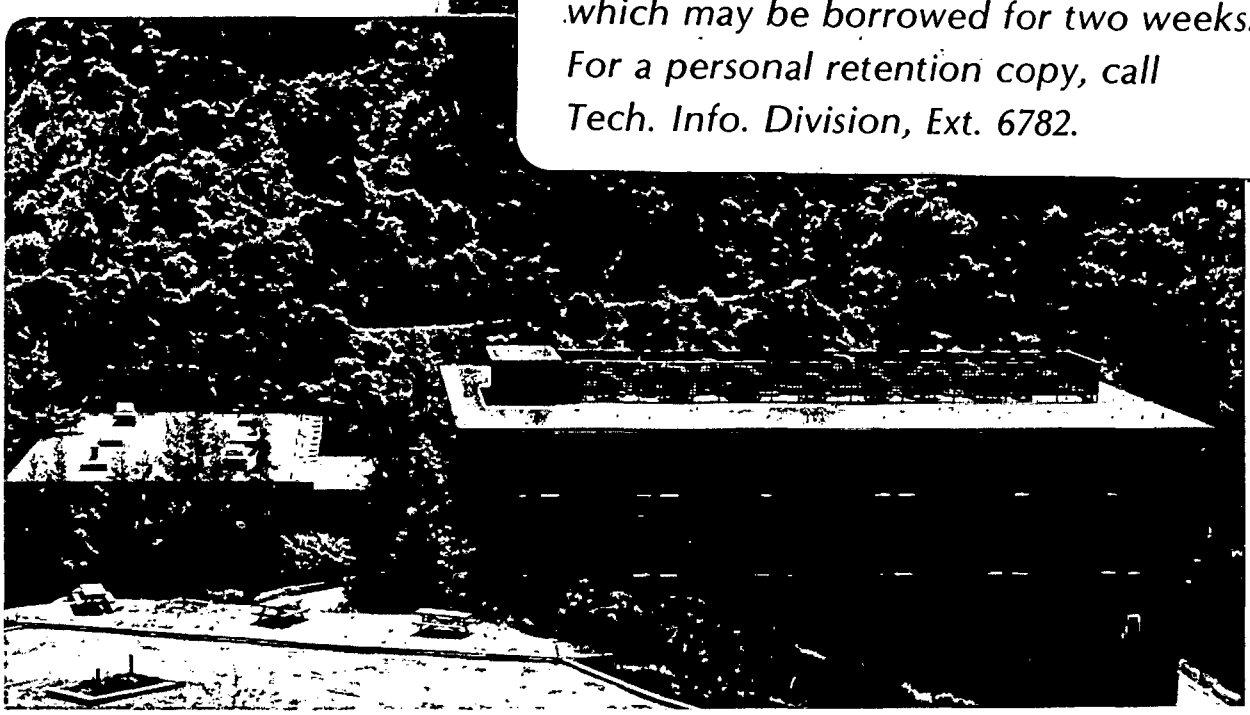

Prepared for the U.S. Department of Energy under Contract DE-AC03-76SF00098

DISCLAIMER

X-RAY ENERGY DISPERSIVE SPECTROSCOPY OF INTERGRANULAR PHASES IN βll β' SIALONS*

T.R. Dinger and G. Thomas

Department of Materials Science and Mineral Engineering,
Materials and Molecular Research Division,
Lawrence Berkeley Laboratory,
University of California,
Berkeley, California 94720

ABSTRACT

X-ray energy dispersive spectroscopy in conjunction with scanning transmission electron microscopy was used to qualitatively and semi-quantitatively characterize retained noncrystalline phases in several compositions of βll β' sialons. Diffuse dark field imaging in conventional transmission mode was used to identify noncrystalline phases prior to x-ray microanalysis. Results show that partitioning of Al and impurity atoms does not occur for these compositions except in isolated cases. In addition, Fe impurities appear to be readily incorporated into the matrix phase.

INTRODUCTION

The use of silicon nitride ceramics for structural components of high temperature gas turbine engines and the problems associated with the fabrication of these ceramics are well documented. Alloying of Si_3N_4 with Al_2O_3 was first proposed in 1972 by Jack[1] in England and Oyama[2] in Japan with the simultaneous discovery of the β' solid solution field in the Si_3N_4-SiO_2-Al_2O_3-AlN system. With this discovery came the realization that single-phase silicon nitride ceramics could theoretically be fabricated by incorporating the transient liquid phase necessary for

*presented at the Advances in Materials Characterization Conference, University Series on Ceramic Science, Alfred University, Alfred, NY, August 16-18, 1982.

densification into the crystalline matrix phase.

Numerous attempts at fabrication have resulted in alloys with properties comparable to those of hot-pressed silicon nitride. However, these alloys still retain various amounts of intergranular phase which degrades the high temperature properties of the ceramic. Retention of this noncrystalline intergranular phase has been attributed to volatilization of N_2 and SiO_3 during fabrication resulting in compositions lying outside the single-phase field, to segregation of impurities in the grain boundary phase[4,5], or to thermodynamic and microstructural restrictions[6].

The purpose of the work presented in this paper was to determine whether segregation of impurities or Al partitioning was occurring, and whether these mechanisms could then be interpreted as a cause for the retention of noncrystalline intergranular phases in low Al β' solid solution alloys.

Because of the very small scale of the intergranular phase pockets (often smaller than 50 nm), analysis using transmission electron microscopy (TEM) and scanning transmission electron microscopy (STEM) in conjunction with x-ray energy dispersive spectroscopy was required to obtain the necessary spatial resolution.

EXPERIMENTAL PROCEDURE

Alloying of Si_3N_4 with Al_2O_3 is a process that is filled with compromise. Large additions of alumina result in readily sinterable ceramics with excellent oxidation resistance[1,7] but with poor thermal shock resistance[8-10]. With this in mind, compositions with low Al content corresponding to β11 (11 eq.% Al^{+3}) where chosen lying close

to the β' solid solution field in the β'ss-Si_2ON_2-X_1 compatibility triangle (see Figure 1). These compositions were chosen to suppress the formation of Si_2ON_2 and the mullite-like X_1 phase, therefore producing an essentially two-phase material containing β' solid solution and retained noncrystalline grain boundary phase.

The results of an emission spectrographic analysis of the Si_3N_4, Al_2O_3, and AlN starting powders appear in Table 1. The powders were weighed, milled, and mixed in an attrition mill with Al_2O_3 balls for 12 hours in n-hexane. The wear of the balls was taken into account in the final composition. The mixed powders were then dried, sieved, and hot-pressed in BN-coated graphite dies under 35 MPa pressure at 1770°C or 1780°C for 45 or 60 minutes. After firing, the surface layer was removed by mechanical grinding, and bulk density measurements were made by the Archimedes method. Phase analyses were made by x-ray diffraction using a Philips goniometer with Cu Kα radiation and a LiF single crystal monochromator. The compositions of the specimens, hot-pressing conditions, and results of the analyses are summarized in Table II. Since composition A did not fully densify, further microstructural analysis was not deemed necessary.

In order to prepare electron transparent thin sections, hot-pressed discs were first thinly sectioned on a diamond wafering saw before being mechanically ground with SiC paper to thicknesses of approximately 50 μm. After attachment to 3 mm copper grids with a Ag-based cement, sections were further thinned by ion milling with 6 KV argon ions at a 20° angle of incidence. A thin layer of carbon was then evaporated onto the surface of the sample to help alleviate the problems

associated with surface charging.

The electron microscopy of compositions B through E was done in a Philips EM400 transmission electron microscope equipped with scanning coils and a Kevex micro-x 7000 analytical spectrometer. Specimens were initially examined in conventional TEM mode using the technique outlined by Krivanek et al.[13] to identify noncrystalline intergranular phases. In this technique, only those electrons which have undergone diffuse scattering by the noncrystalline phase are allowed to form the image. Thus, the noncrystalline regions appear light on a dark background in dark field.

After the initial identification of intergranular phase pockets of sufficient size for x-ray microanalysis, the microscope was switched to scanning mode using a nominal probe size of 10 nm. All microscopy was done using electrons of 100 KeV incident energy. X-ray spectra[14] were obtained in the energy range of 0 to 10.24 KeV with a channel width of 10 eV. Spectra were acquired by count integration on the Si K_α peak. These integrations were for 10K, 20K, 50K, or 100K counts, with normal acquisition times being 300 to 350 seconds per 1024 channel spectrum depending on the thickness of the specimen. This technique permitted analyses for all elements of interest except nitrogen and oxygen.

DISCUSSION OF RESULTS

The initial examination of the series in conventional transmission mode resulted in the bright field/dark field micrograph pairs of Figure 2 through Figure 5, representing compositions B through E, respectively. As would be expected from the composition data and Figure 1, the amount

of noncrystalline phase and the size of noncrystalline phase pockets increases in the series moving from composition B to composition E. These grain boundary phases appear in light contrast in the dark field micrographs with the larger pockets being labeled (g).

The results of nearly 80 comparative spectra are represented, for the most part, by Figure 6 through Figure 10. As can easily be seen from Figure 6, very little, if any, distinction can be made between the spectra corresponding to the noncrystalline intergranular phase (solid line) and to the crystalline phase (dots). This tendancy was strong in all four compositions examined indicating that little or no partitioning of Al had occurred. The Cr and Cu peaks apparent in all specta are systems background and will not be treated further[15]. Note that the Fe impurity peak appears with equal intensity in both the crystalline matrix phase and the noncrystalline intergranular phase. The equivalent Si/Al ratios hint at different O/N ratios between phases as a reason for retention of the noncrystalline grain boundary phase.

The comparative spectra of Figure 7 illustrate one of the rare instances where Ca impurities were found to be segregated in the grain boundary phase (dots)[16,17]. Even in this case, the Ca peak is barely significant above background, but is definitely of higher intensity than that of the crystalline matrix phase (solid line). This effect was not apparent in the remainder of the sample or in other compositions of the series.

The spectra of Figure 8 illustrate one of several instances in which the noncrystalline phase was found to be rich in Si. One possible explanation for this is that the crystalline phase probed corresponded to

an X_1 phase grain exhibiting a much higher Al content. This does not seem probable, however, due to the distinctive elongated and often twinned morphology[18] of the X_1 phase which was not observed. A simpler and more acceptable explanation is that a local inhomogeneity has resulted in the noncrystalline phase being enriched with Si.

The STEM micrograph of Figure 9 illustrates Fe-rich inclusions (arrowed and in dark contrast) which have perhaps provided the most interesting results of the investigation. The comparative spectra of Figure 10 arise from the Fe-rich inclusion (arrow), the adjacent non-crystalline intergranular phase (-), and the adjacent crystalline matrix phase (..). Jack[19] has indicated that incorporation of impurities such as Ca and Mg into the sialon phase could occur in much the same way as the substitution of Al as long as charge neutrality is maintained. The homogeneous distribution of Fe in both the matrix and intergranular phases may indicate that this argument should be extended to include Fe impurities as well. Fe-rich inclusions of this type were found only in composition E, but in each case, the spectra were similar to those of Figure 9.

CONCLUSIONS

The four β11 β' sialon compositions examined by transmission electron microscopy, scanning transmission electron microscopy, and x-ray energy dispersive spectroscopy were found to contain various amounts of non-crystalline intergranular phase depending on the composition used. The amount of intergranular phase present increased, as expected, with increasing oxygen/nitrogen ratio. X-ray energy dispersive spectroscopy indicated that all compositions were homogeneous with respect to silicon/aluminum ratios between crystalline matrix and non-crystalline grain

boundary phases with few exceptions noted. Impurity distributions were found to be equally homogeneous with the exception of Ca which tended to segregate in noncrystalline grain boundary phases. This is in contrast to earlier investigations which have found the intergranular phase to be a sink for several types of impurity atoms. In addition, localized Fe impurities have been found to be accommodated by both the matrix and intergranular phases in a homogeneous manner. This lends support to Jack's theory that impurity phases may be incorporated into the matrix in these solid solution materials.

ACKNOWLEDGEMENTS

This work was supported by the National Science Foundation under grant number DMR-77-24022 with facilities and support staff provided by the Director, Office of Energy Research, Office of Basic Energy Sciences, Division of Materials Sciences of the U.S. Department of Energy under contract number DE-AC03-76SF00098. Thanks go to Dr. J. Weiss and Dr. P. Greil of the Max-Planck-Institut für Metallforschung Institut für Werkstoffwissenschaften, for providing the sample material and supporting analysis data.

REFERENCES

1. K.H. Jack and W.I. Wilson, Ceramics Based on the Si-Al-O-N and Related Systems, Nature (London), Phys. Sci. 238:28-29 (1972).
2. Y. Oyama and O. Kamagaito, Hot-Pressing of Si_3N_4-Al_2O_3, Yogyo Kyokai Shi 80:327-336 (1972).
3. K.H. Jack, The Relationship of Phase Diagrams to Research and Development of Sialons, in, "Phase Diagrams: Materials Science and Technology, Volume 6-V: Crystal Chemistry, Stoichiometry, Spinoidal Decomposition, Properties of Inorganic Phases," A.M. Alper, ed., Academic Press, San Francisco (1978).
4. D.R. Clarke, The Microstructure of a 12H Mg-Si-Al-O-N Polytype Alloy: Intergranular Phases and Compositional Variations, J. Am. Cer. Soc., 63: 208-214 (1980).
5. O.L. Krivanek, T.M. Shaw and G. Thomas, The Microstructure and Distribution of Impurities in Hot-Pressed and Sintered Silicon Nitrides, J. Am. Cer. Soc., 62:585-590 (1979).
6. R. Raj and F.F. Lange, Crystallization of Small Quantities of Glass (or a Liquid) Segregated in Grain Boundaries, Acta. Met. 29:1993-2000 (1981).
7. S.C. Singhal and F.F. Lange, Oxidation Behavior of Sialons, J. Am. Cer. Soc., 60:190-191 (1977).
8. F.F. Lange, H.J. Siebeneck, and D.P.H. Hasselman, Thermal Diffusivity of Four Si-Al-O-N Compositions, J. Am. Cer. Soc. 59: 454-455 (1976).

9. M. Kariyama, Y. Inomata, T. Kujima, and Y. Hasegawa, Thermal Conductivity of Hot-Pressed Si_3N_4 by the Laser Flash Method, Bull. Am. Cer. Soc. 57:1119-1122 (1978).

10. F.F. Lange, Silicon Nitride Alloy Systems: Fabrication, Microstructure and Properties, Rockwell International Science Center, Report No. J1376A/SN.

11. I.N. Naik, L.J. Gauckler, and T.Y. Tien, Solid-Liquid Equilibria in the System Si_3N_4-AlN-SiO_2-Al_2O_3, J. Am. Cer. Soc. 61: 332-335 (1978).

12. P. Greil and J. Weiss, Evaluation of the Microstructure of β Solid Solution Materials with 11 Eq. % Al^{+3} Containing Different Amounts of Amorphous Grain Boundary Phases, to be published.

13. O.L. Krivanek, T.M. Shaw and G. Thomas, Imaging of Thin Intergranular Phases by High Resolution Electron Microscopy, J. Appl. Phys. 50:4223-4227 (1979).

14. See for instance, "Introduction to Analytical Electron Microscopy," J.J. Hren, J.I. Goldstein, and D.C. Joy, eds., Plenum Publishing Corporation, New York (1979).

15. J. Bentley, Systems Background in X-ray Microanalysis, in: "Analytical Electron Microscopy-1981," R.H. Geiss, ed., San Francisco (1981).

16. M.H. Lewis, B.D. Powell, P. Drew, R.J. Lumby, B. North, and A.J. Taylor, The Formation of Single-Phase Si-Al-O-N Ceramics, J. Mat. Sci. 12:61-74 (1977).

17. D.R. Clarke, N.J. Zaluzec, and R.W. Carpenter, The Intergranular Phase in Hot-Pressed Silicon Nitride: I, Elemental Composition, J. Am. Cer. Soc. 64:601-607 (1981).

18. A. Zangvil, The Structure of the X phase in the Si-Al-O-N Alloys, J. Mat. Sci. 13:1370-1374 (1978).

19. K.H. Jack, The Crystal Chemistry of the Sialons and Related Nitrogen Ceramics, in: "Nitrogen Ceramics," F.L. Riley, ed., Noordhoff International Publishing, Leyden, The Netherlands (1977).

Fig. 1. Isothermal section of the Si-Al-O-N system at 1750°C after Naik et al.[11]. Compositions B, C, D, and E were used in the investigation.

Fig. 2. Bright field/dark field pair of composition B. Note noncrystalline phases which appear in light contrast in dark field and are labeled (g).

Fig. 3. Bright field/dark field pair in composition C. Noncrystalline grain boundary phases are denoted by (g).

Fig. 4. Bright field/dark field pair of composition D. Noncrystalline phases are denoted by (g).

Fig. 5. Bright field/dark field pair of composition E. Noncrystalline phases are denoted by (g).

Fig. 6. Typical comparative spectra of the four compositions analyzed. The intergranular phase is denoted by (—) while the crystalline phase is denoted by (...).

Fig. 7. Nontypical comparative spectra for composition D illustrating a very slight Ca enrichment in the noncrystalline intergranular phase.

Fig. 8. Nontypical comparative spectra for composition E illustrating an apparent enrichment of the noncrystalline phase (—) with Si.

Fig. 9. STEM micrograph of Fe-rich inclusions and surrounding microstructure in composition E.

Fig. 10. Comparative spectra for Fe-rich inclusion (arrow) and surrounding crystalline (—) and noncrystalline (..) phases in composition E.

TABLE 1

Chemical Composition of Starting Powders*

Element	Amount Present (wt.%)		
	α-Si_3N_4 Starck, Berlin HCST 3510	AlN Starck, Berlin HCST 530	Al_2O_3 Alcoa A 16
Si_{total}	60.1	-	-
Al	0.06	65.03	52.9
O	2.0	3.12	47.04
N	37.1	31.85	-
Fe	0.01	-	-
K	0.001	-	-
C	0.4	-	-
Ca	0.03	-	-
Ti	0.002	-	-
Li	0.0005	-	-
Si_{free}	0.5	-	-
Mg	0.003	-	0.06
Na	0.003	-	-
W	0.01	-	-

*Emission spectroscopy. Data provided by Dr. J. Weiss and Dr. P. Greil, Max-Planck Institut für Metallforschung, Stuttgart, West Germany[12].

TABLE II.

Chemical Compositions, Hot-Pressing Conditions, Bulk Density, and Phase Compositions of Sialons Examined**

	Eq. %				Temp. (°C)	Time (min.)	Density (g/cm^3)	Phases (XRD)
	Si	Al	O	N				
A	89.4	10.6	7.5	92.5	1780	60	2.67	β'ss, Si_2ON_2
B	89.4	10.6	9.2	90.8	1770	45	3.150	β'ss, Si_2ON_2
C	89.4	10.6	10.9	89.1	1770	45	3.136	β'ss, Si_2ON_2
D	89.4	10.6	12.6	87.4	1770	45	3.116	β'ss, Si_2ON_2, $^2X_1$
E	89.4	10.6	14.0	86.0	1770	45	3.103	β'ss, Si_2ON_2, X_1

**Data provided by Dr. J. Weiss and Dr. P. Greil, Max-Planck-Institut für Metallforschung, Stuttgart, West Germany[12].

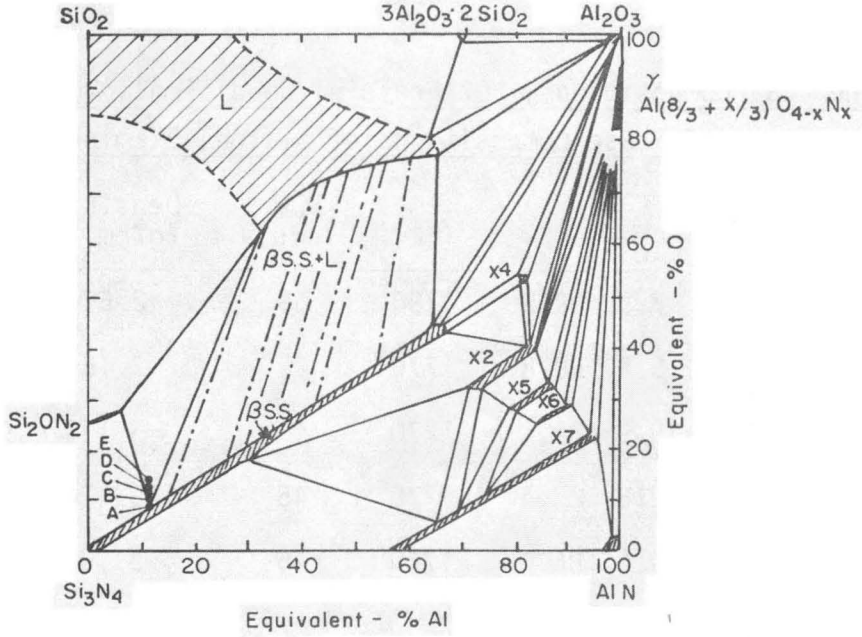

Fig. 1

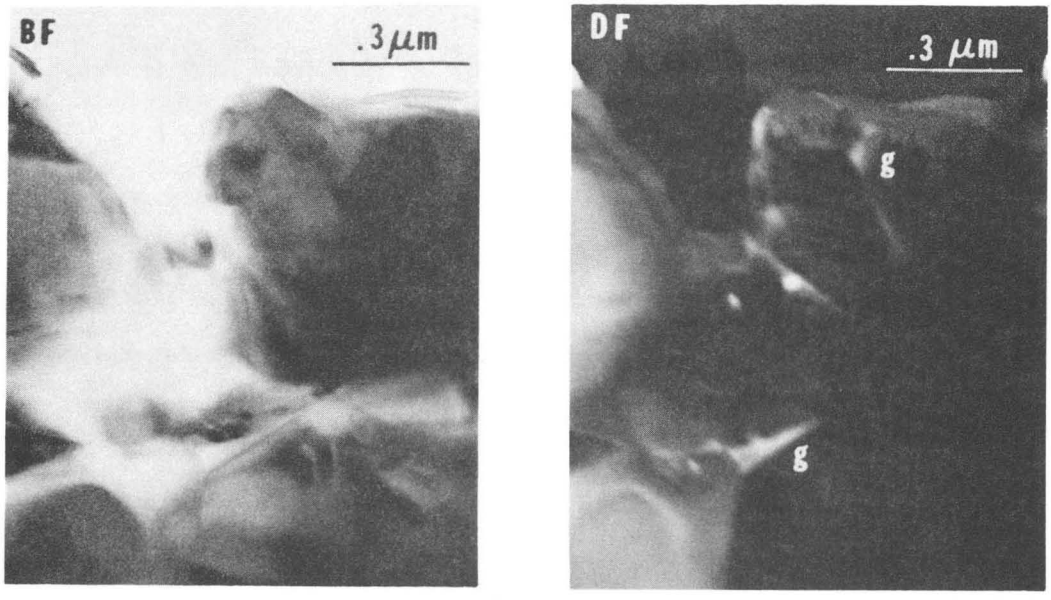

XBB 828-06916

Fig. 2

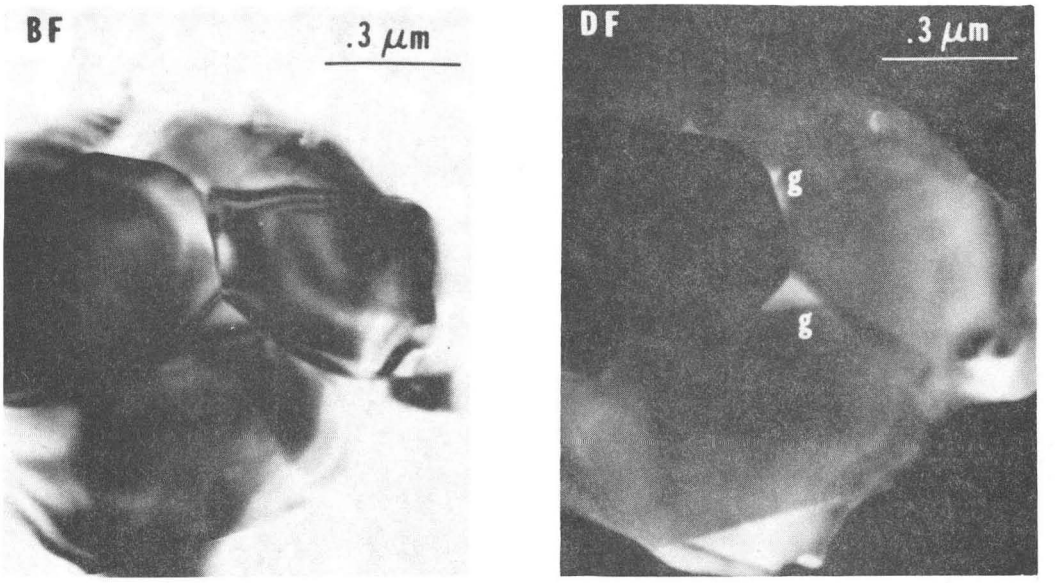

XBB 828-06917

Fig. 3

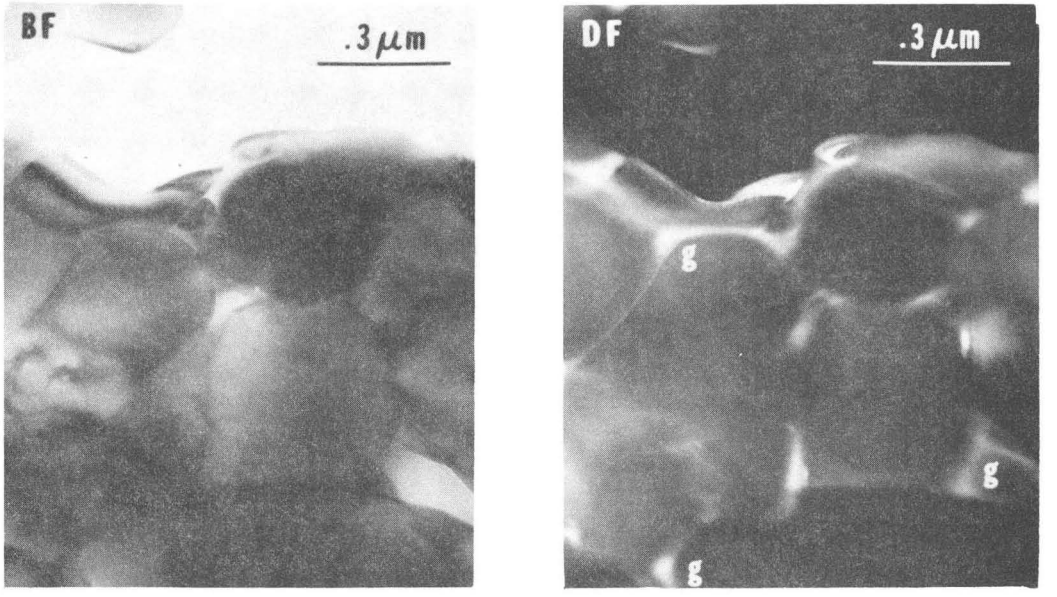

XBB 828-06918

Fig. 4

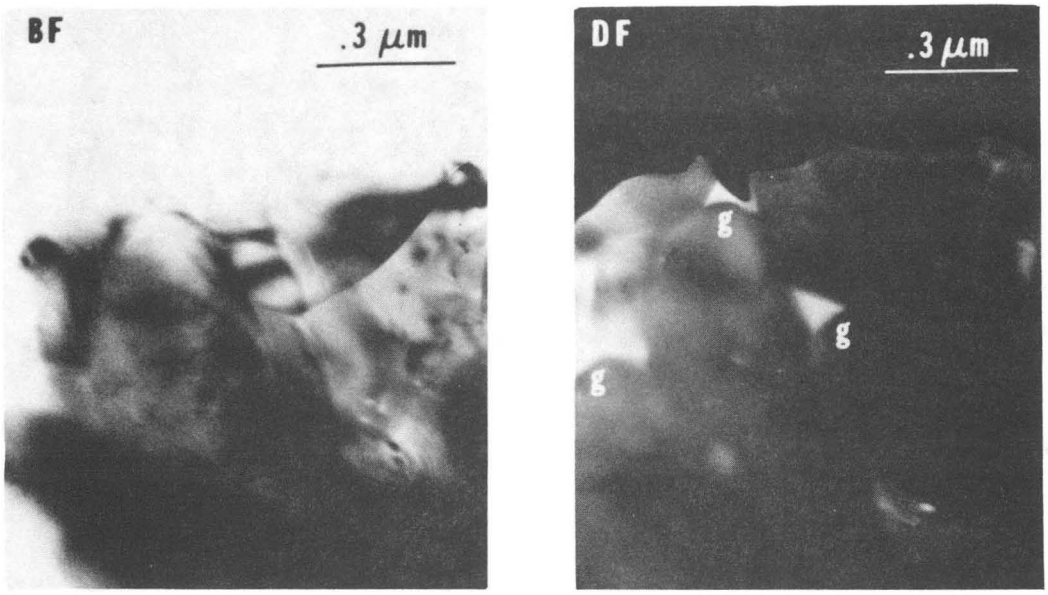

XBB 828-06919

FIg. 5

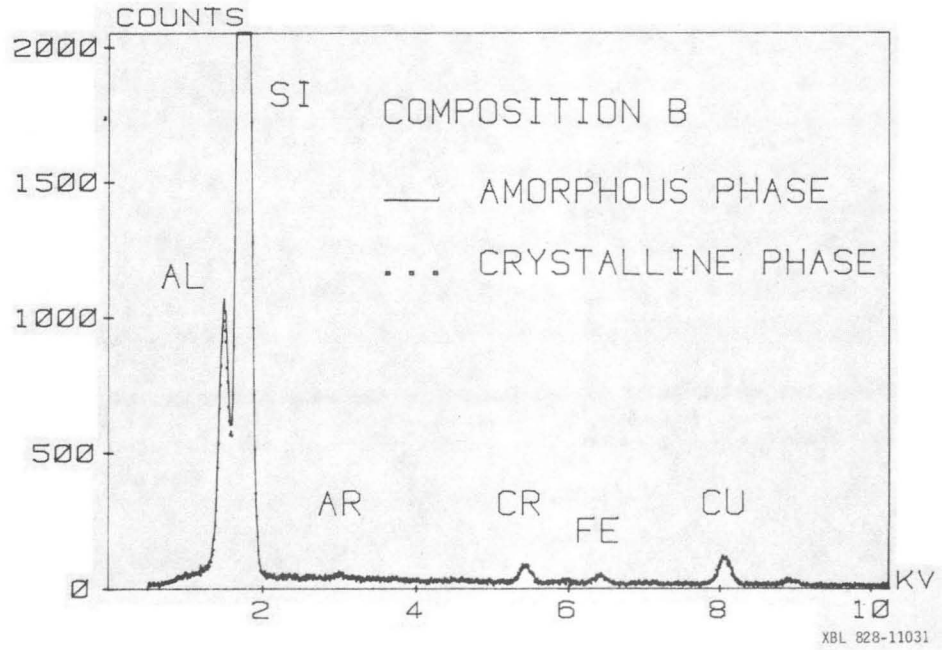

Fig. 6

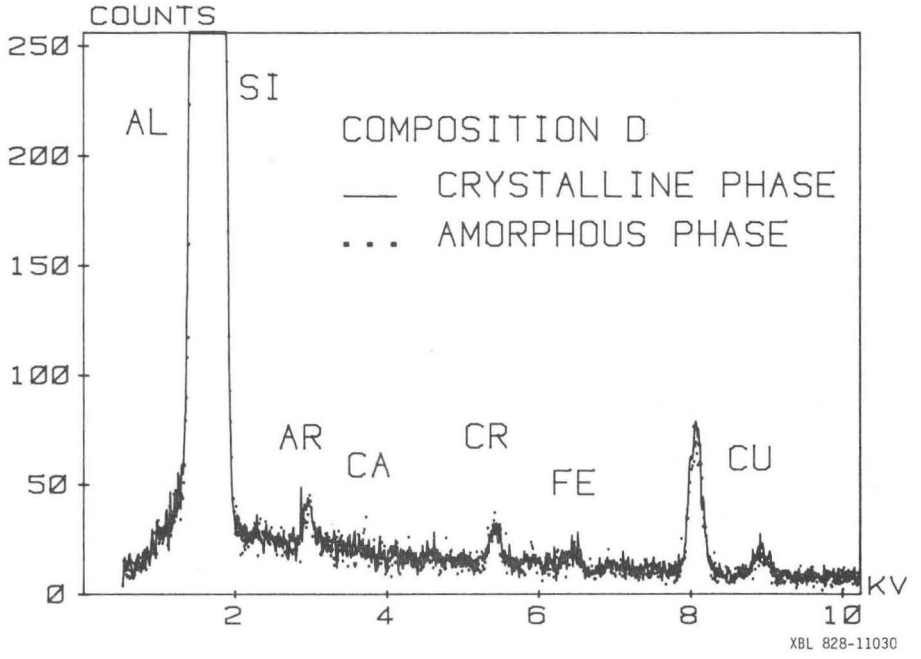
COUNTS
250
200
150
100
50
0
AL
SI
COMPOSITION D
___ CRYSTALLINE PHASE
... AMORPHOUS PHASE
AR
CA
CR
FE
CU
KV
2
4
6
8
10
XBL 828-11030

Fig. 7

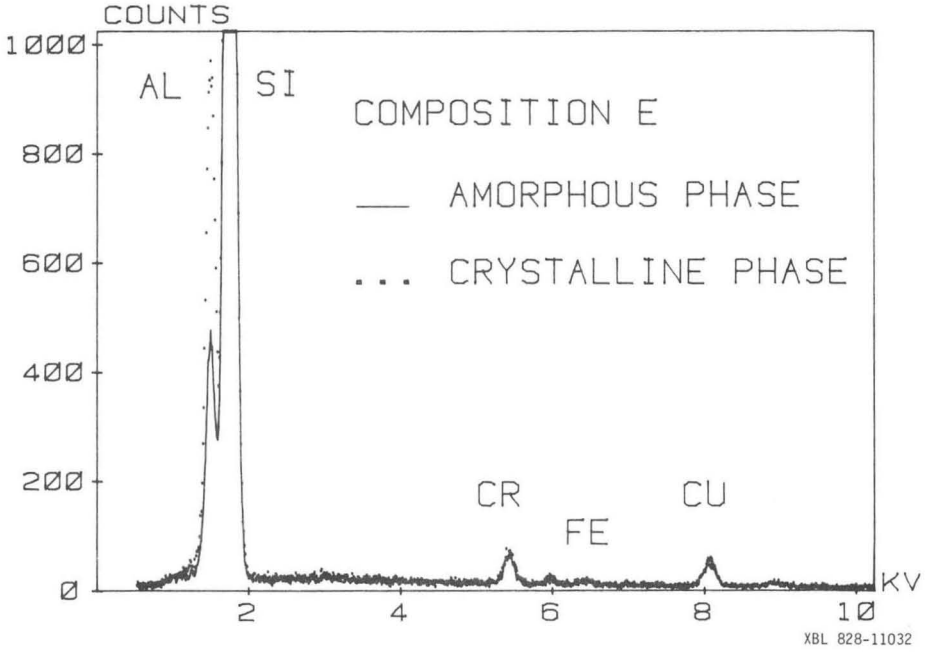
COUNTS
1000
800
600
400
200
0
AL
SI
COMPOSITION E
___ AMORPHOUS PHASE
... CRYSTALLINE PHASE
CR
FE
CU
KV
2
4
6
8
10
XBL 828-11032

Fig. 8

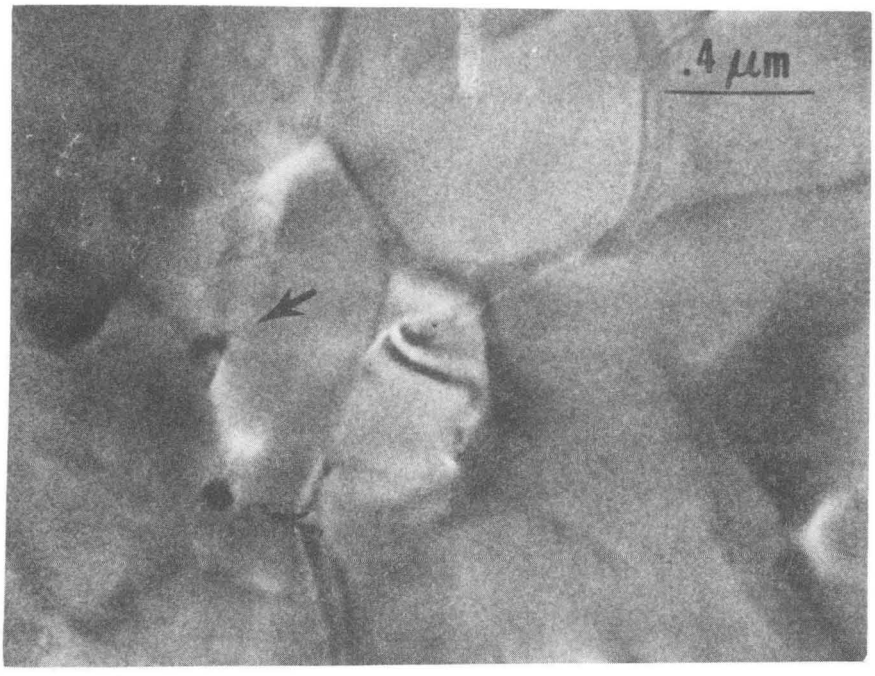

XBB 828-06920

Fig. 9

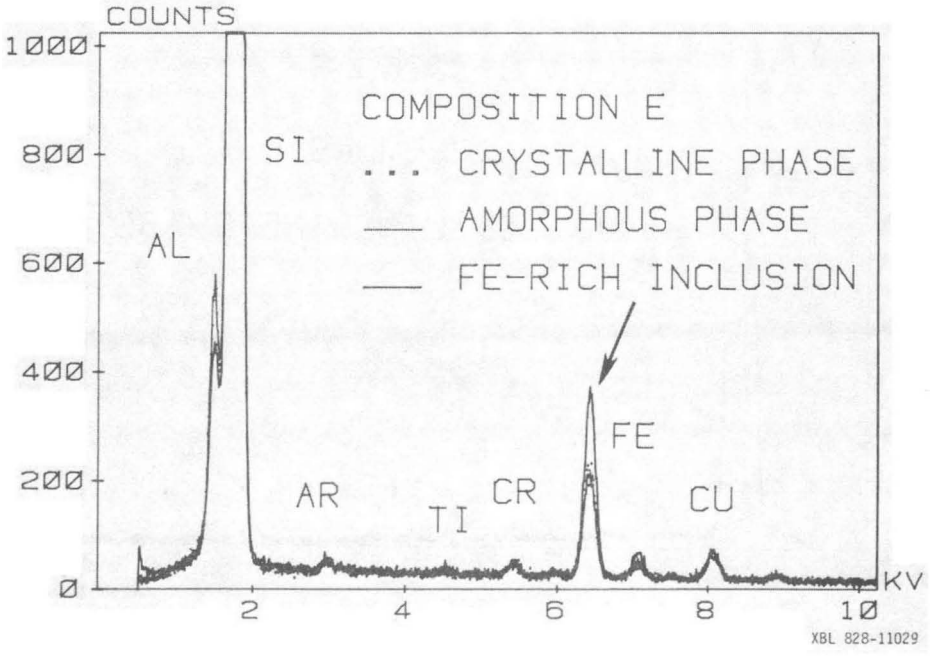

Fig. 10

This report was done with support from the Department of Energy. Any conclusions or opinions expressed in this report represent solely those of the author(s) and not necessarily those of The Regents of the University of California, the Lawrence Berkeley Laboratory or the Department of Energy.

Reference to a company or product name does not imply approval or recommendation of the product by the University of California or the U.S. Department of Energy to the exclusion of others that may be suitable.

TECHNICAL INFORMATION DEPARTMENT
LAWRENCE BERKELEY LABORATORY
UNIVERSITY OF CALIFORNIA
BERKELEY, CALIFORNIA 94720